# Effects of Spatial Constraint on Clustering-Based Sea-Surface Observation Targeting for Typhoon Forecasting

Yusuke Umemiya[1], Kosuke Ito[3, 2], Naoko Kosaka[1, 2], Tsuneko Kura[1], Toshiyuki Bandai[1], Gota Yamasaki[1], Hiroshi Matsubara[1], Satoshi Mitarai[4, 2], Daiki Suzuki[2] and Hironori Fudeyasu[2]

[1]NTT, Inc., Japan; [2]Typhoon Science and Technology Research Center, Yokohama National University, Japan; [3]Kyoto University, Japan; [4]Okinawa Institute of Science and Technology Graduate University, Japan

2026-08-25
SynObs & Ocean Observing Co-Design, Joint International Workshop

© NTT, Inc. 2026

# Motivation and research question (RQ)

**Where should limited ocean observations be deployed?**

With only a few observing platforms, we need locations with high forecast impact and low spatial redundancy.

Toward a sustained ocean observing network

↓

Limited observing platforms must be deployed effectively

↓

Here, we consider five sea-surface observing platforms

↓

Where should we observe to improve typhoon forecasts?

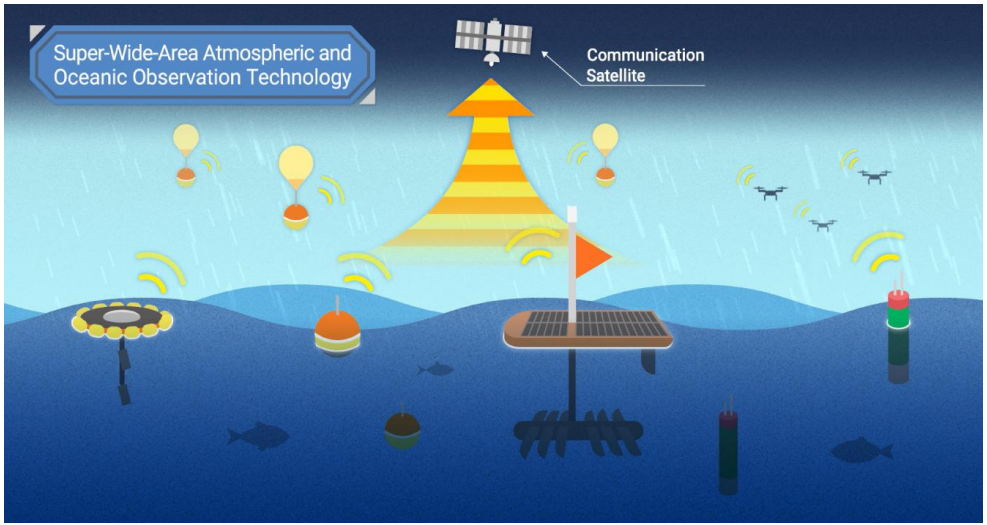



Fig. 1. Concept of the proposed marine observation network

RQ: Can we use forecast sensitivity to identify a practical five-site observing configuration?

© NTT, Inc. 2026

# Proposed targeting methods

**From adjoint sensitivity to five observation sites**

Adjoint sensitivity identifies forecast-relevant regions, and clustering selects five spatially distributed representative sites.

Initial pressure sensitivity $S = \frac{\partial J}{\partial P_0}$ (Fig. 2a)

$\left( J = \frac{1}{N_{100}} \sum_{(i,j) \in A_{100}} P(i, \mathrm{j}, k = 1) \right)$

↓

Strong-wind region (10-m wind speed ≥ 15 $^{\mathrm{m}}/_{\mathrm{s}}$)
(Spatial constraint)

↓

Top 10% absolute sensitivity |S| (Fig. 2b)

↓

Clustering: k-medoids

↓

Five observation sites (Fig. 2c)

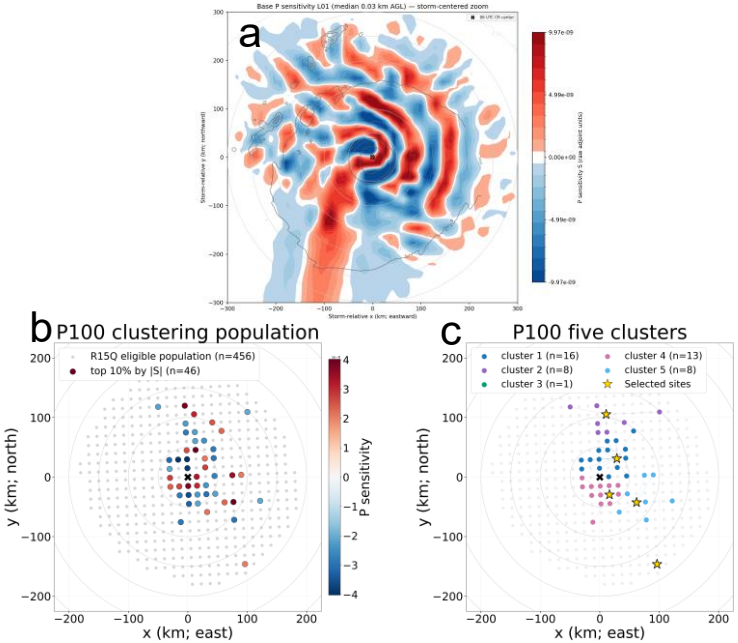



Fig. 2. Clustering of high-sensitivity candidates. (a) Sensitivity field. (b) Top-10% candidates. (c) Five clusters and selected medoid sites.

© NTT, Inc. 2026

# Experimental design: Two typhoon OSSEs

**Perfect-model OSSEs for two contrasting typhoons**

We test the five-site strategy in two perfect-model OSSEs using 3DVAR and 6-h forecasts for two typhoon cases (Hinnamnor (2022) and Trami (2018)).

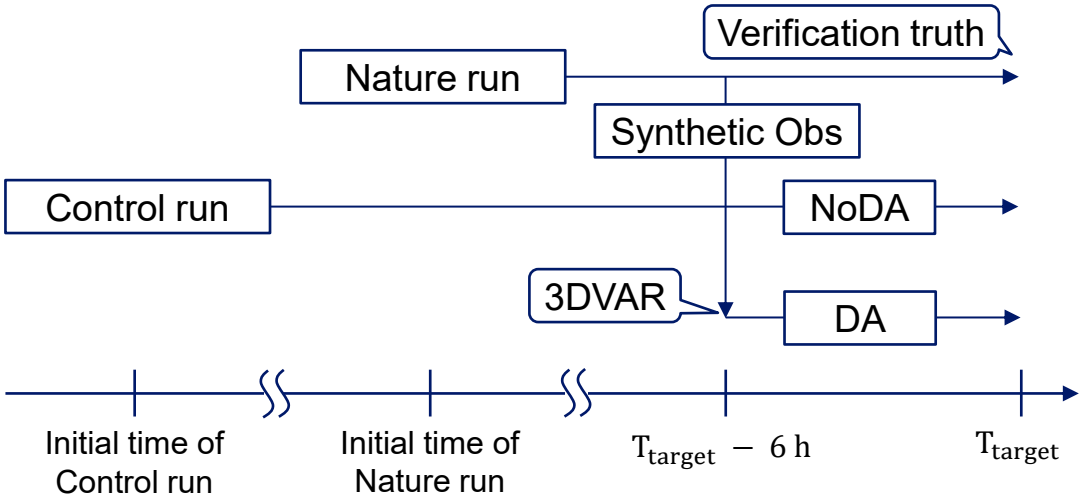



Fig. 3. OSSE workflow.

Table. 1. Experimental configuration

| | |
|---|---|
| Model | WRF-ARW / WRFDA v4.5.2 |
| Case | Hinnamnor (2022)<br>Trami (2018) |
| IC/BC | NCEP GDAS/FNL 0.25 deg analyses, 6-hourly |
| Domain and grids | d01 (15 km): adjoint sensitivity + 3DVAR<br>d02 (3 km): forecast verification |
| Synthetic observations | Pressure (P), Temperature (T) and zonal and meridional wind components (U, V) at five sites, noise-free |

© NTT, Inc. 2026

# Four observation-location strategies

**Four strategies isolate the value of sensitivity information**

We compare the proposed method (P100) with low-sensitivity (LOW), near-core (NEARCORE) and geometry-matched random observations (RANDOM) to separate sensitivity from location effects.

Table. 2. Targeting configurations and their experimental roles

| Method | Selection-rule | Role |
|---|---|---|
| P100 | Top 10% of $\|S\|$ + clustering | Proposed |
| LOW | Bottom 10% of $\|S\|$ + clustering | Sensitivity control |
| NEARCORE | Five eligible sites nearest the storm center | Distance control |
| RANDOM | Same radial bins and quadrants as P100; $\geq 30$ km separation; n=30 | Geometry control |

© NTT, Inc. 2026

# Result: Hinnamnor case

**From selected observation sites to forecast response**

The five-site assimilation produces only a small response in minimum pressure, with a slight error reduction emerging by the 6-h verification time.

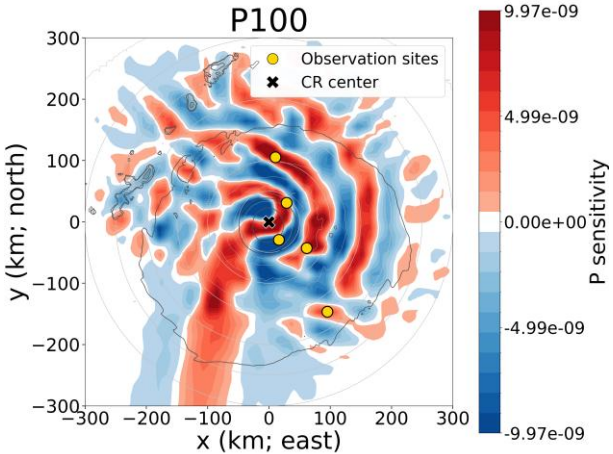



Fig. 4. Selected observation sites for P100.

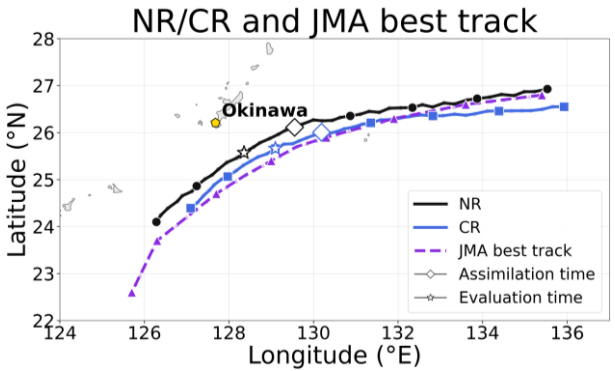



Fig. 5.TC tracks of NR/CR and JMA best track.

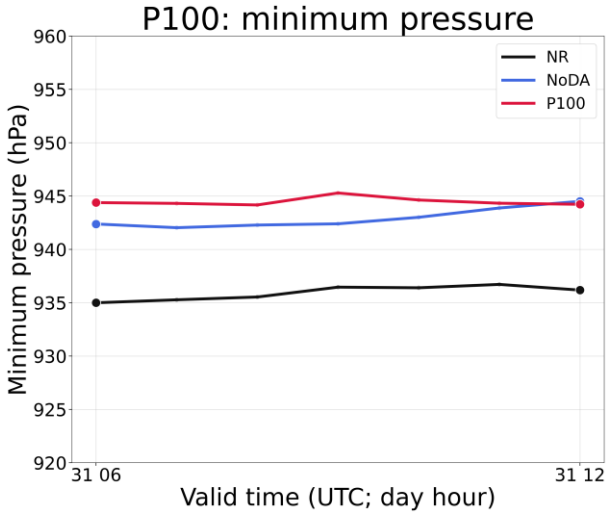



Fig. 6. Minimum pressure timeseries of NR, NoDA (=CR) and P100.

© NTT, Inc. 2026

# Impact on typhoon intensity

: Both metrics improved

**P100 slightly reduces both intensity errors in both cases**

P100 reduces errors in both minimum pressure and maximum wind for Hinnamnor and Trami, although the improvements are small. LOW does not improve both metrics, while RANDOM shows mixed impacts.

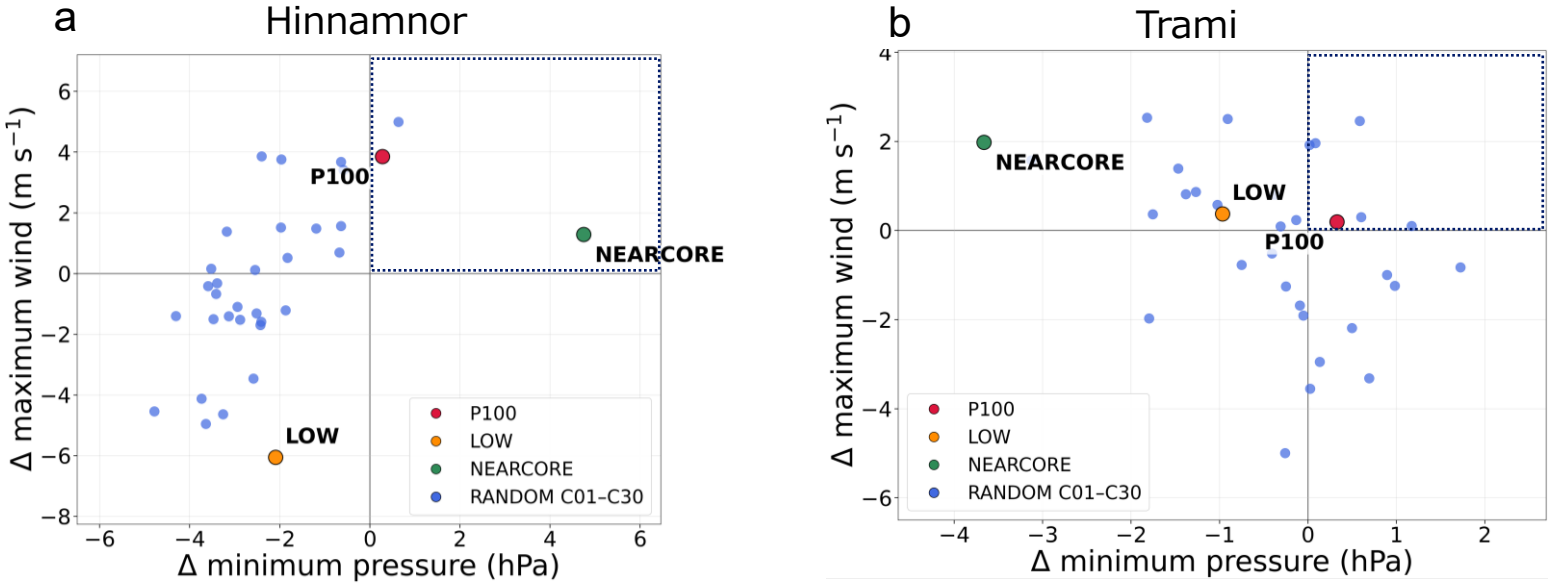


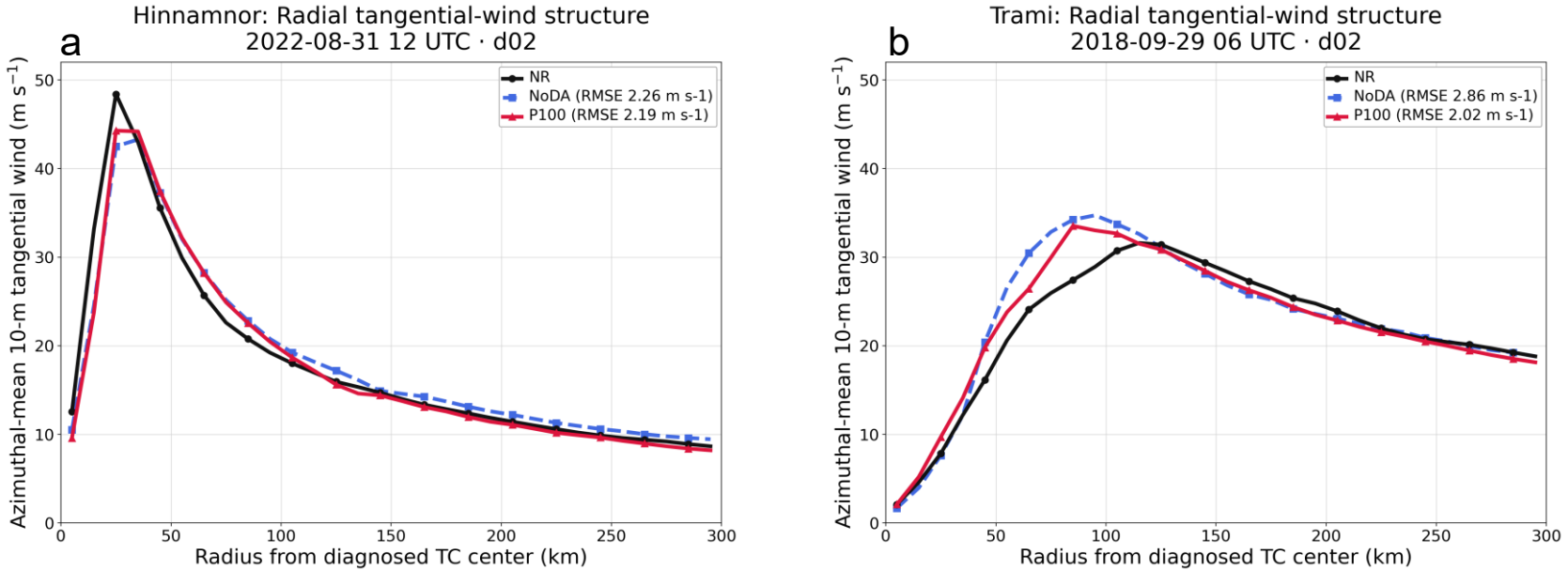

Fig. 7. Forecast improvement relative to NoDA for each targeting configuration: (a) Hinnamnor and (b) Trami. Positive values indicate reduced error against the nature run.

© NTT, Inc. 2026

# Impact on typhoon structure

**P100 reduces errors in the radial tangential-wind profile, particularly in Trami**

P100 slightly reduces the radial tangential-wind RMSE in Hinnamnor and more clearly reduces it in Trami, especially in the inner-core region around 50–100 km from the storm center.
RMSE: Hinnamnor: $2.26\ ^{m}/_{s} \rightarrow 2.19\ ^{m}/_{s}$; Trami: $2.86\ ^{m}/_{s} \rightarrow 2.02\ ^{m}/_{s}$




© NTT, Inc. 2026

Fig. 8. Radial profiles of tangential wind averaged azimuthally in 10-km radial bins: (a) Hinnamnor and (b) Trami.

# Interpretation and limitations

**Why is the response larger for Trami?**

The larger improvement in Trami may reflect an interaction between its broader vortex and the spatially broad increments produced by the current 3DVAR background-error setting.

Broader vortex
+
Broad 3DVAR increment
↓
Larger forecast response?

Interpretation — not yet demonstrated

- only two cases
- default background-error covariance
- relatively small absolute correction
- horizontal correlation scale experiments underway

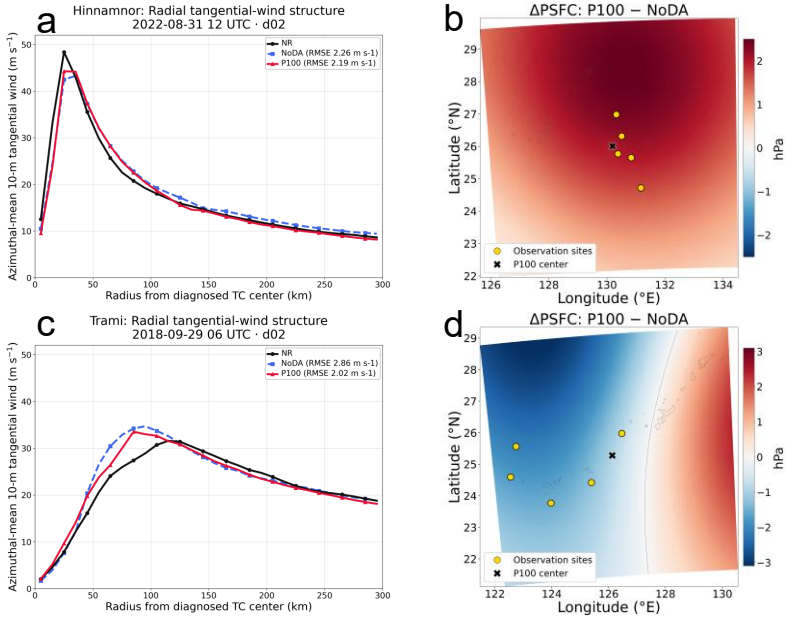



Fig. 9. Comparison of storm structure and analysis increments: (a, b) Hinnamnor and (c, d) Trami.

© NTT, Inc. 2026

# Conclusions and next steps

**Conclusions**

1. Adjoint sensitivity and clustering with spatial constraint provide a deterministic way to select five spatially distributed, forecast-relevant observation sites.

2. The proposed sites **slightly reduced errors in both minimum pressure and maximum wind** in Hinnamnor and Trami, while LOW did not reduce both errors and RANDOM showed mixed impacts.

3. P100 also **reduced the RMSE of the radial tangential-wind profile in both cases, with a larger reduction in Trami**, while the dependence on DA configuration and storm characteristics remains to be evaluated.

**Next:** additional cases × background-error sensitivity × observation number / variables

Thank you for your attention.

© NTT, Inc. 2026